Appendix A. Supplementary data

Supplementary data associated with this article can be found, in the online version, at http://dx.doi.org/10.1016/j.jdermsci.2015.10.015.

References

[1] M.L. Dorfman, C. Hershko, S. Eisenberg, F. Sagher, Ichthyosiform dermatosis with systemic lipidosis, Arch. Dermatol. 110 (1974) 261–266.
[2] I. Chanarin, A. Patel, G. Slavin, E.J. Wills, T.M. Andrews, G. Stewart, Neutral-lipid storage disease: a new disorder of lipid metabolism, Br. Med. J. 1 (1975) 553–555.
[3] C. Lefevre, F. Jobard, F. Caux, B. Bouadjar, A. Karaduman, R. Heilig, et al., Mutations in CGI-58, the gene encoding a new protein of the esterase/lipase/thioesterase subfamily, in Chanarin-Dorfman syndrome, Am. J. Hum. Genet. 69 (2001) 1002–1012.
[4] T. Takeichi, L. Liu, K. Fong, L. Ozoemena, J.R. McMillan, A. Salam, et al., Whole-exome sequencing improves mutation detection in a diagnostic epidermolysis bullosa laboratory, Br. J. Dermatol. 172 (2015) 94–100.
[5] N. Schleinitz, J. Fischer, A. Sanchez, V. Veit, J.R. Harle, J.F. Pelissier, Two new mutations of the ABHD5 gene in a new adult case of Chanarin Dorfman syndrome: an uncommon lipid storage disease, Arch. Dermatol. 141 (2005) 798–800.
[6] A. Lass, R. Zimmermann, G. Haemmerle, M. Riederer, G. Schoiswohl, M. Schweiger, et al., Adipose triglyceride lipase-mediated lipolysis of cellular fat stores is activated by CGI-58 and defective in Chanarin-Dorfman syndrome, Cell Metab. 3 (2006) 309–319.
[7] M. Akiyama, D. Sawamura, Y. Nomura, M. Sugawara, H. Shimizu, Truncation of CGI-58 protein causes malformation of lamellar granules resulting in ichthyosis in Dorfman-Chanarin syndrome, J. Invest. Dermatol. 121 (2003) 1029–1034.
[8] K. Sugiura, Y. Suga, M. Akiyama, Dorfman-Chanarin syndrome without mental retardation caused by a homozygous ABHD5 splice site mutation that skips exon 6, J. Dermatol. Sci. 75 (2014) 199–201.
[9] R.M. Pujol, M. Gilaberte, A. Toll, L. Florensa, J. Lloreta, M.A. Gonzalez-Ensenat, et al., Erythrokeratoderma variabilis-like ichthyosis in Chanarin-Dorfman syndrome, Br. J. Dermatol. 153 (2005) 838–841.
[10] S. Aggarwal, J.S. Maras, S. Alam, R. Khanna, S.K. Gupta, A. Ahuja, Novel nonsense mutation of ABHD5 in Dorfman-Chanarin syndrome with unusual findings: a challenge for genotype–phenotype correlation, Eur. J. Med. Genet. 55 (2012) 173–177.

Takuya Takeichi[a,b]
[a]Department of Dermatology, Nagoya University Graduate School of Medicine, 65 Tsurumai-cho, Showa-ku, Nagoya 466-8550, Japan, [b]St John's Institute of Dermatology, King's College London, Guy's Hospital, Great Maze Pond, London SE1 9RT, UK

Kazumitsu Sugiura
Department of Dermatology, Nagoya University Graduate School of Medicine, 65 Tsurumai-cho, Showa-ku, Nagoya 466-8550, Japan

Simon Tso
St John's Institute of Dermatology, King's College London, Guy's Hospital, Great Maze Pond, London SE1 9RT, UK

Michael A. Simpson
Division of Genetics and Molecular Medicine, King's College London, Guy's Hospital, Great Maze Pond, London SE1 9RT, UK

John A. McGrath
St John's Institute of Dermatology, King's College London, Guy's Hospital, Great Maze Pond, London SE1 9RT, UK

Masashi Akiyama*
Department of Dermatology, Nagoya University Graduate School of Medicine, 65 Tsurumai-cho, Showa-ku, Nagoya 466-8550, Japan

* Corresponding author. Fax: +81 52 744 2318.
E-mail address: makiyama@med.nagoya-u.ac.jp (M. Akiyama).

Received 14 October 2015
Received in revised form 17 November 2015
Accepted 26 November 2015

http://dx.doi.org/10.1016/j.jdermsci.2015.10.015

Letter to the Editor

Percutaneous exposure to high-dose hapten induces systemic immunosuppression through the inhibition of dendritic cell migration

While sensitization with the optimal dose of an antigen induces antigen-specific T-cell responses, the immune response to a supraoptimal dose of antigen is suppressed [1]. In addition, high-dose antigen exposure under certain conditions suppresses subsequent immune response to the antigen [2,3]. The mechanisms underlying high-dose antigen-induced immunosuppression appear to vary according to the administration route of the high-dose antigen: intravenous injection of high-dose hapten induces suppressor cells [2], while oral administration of high-dose hapten induces anergy or deletion of antigen-specific T cells [3].

Percutaneous sensitization of mice with an optimal dose of haptens such as dinitrofluorobenzene (DNFB), trinitrochlorobenzene (TNCB), and oxazolone induces hapten-bearing dendritic cell (DC) migration from sensitized skin into the draining lymph node (dLN), leading to the proliferation and differentiation of the hapten-specific interferon (IFN)-γ-producing $CD8^+$ effector T (Tc1) cells. Re-exposure to the relevant hapten five days after sensitization elicits allergic contact hypersensitivity (CHS) response by antigen-specific Tc1 cells [4]. A previous report has shown that topical high-dose hapten application induces dysfunction of DCs at hapten-applied sites, resulting in the impaired capacity of hapten-applied skin to support subsequent CHS induction by an optimal sensitizing dose of another hapten [5]. However, it remains unclear whether and how percutaneous exposure to high-dose antigen inhibits subsequent immune responses systemically. In this study, we investigated the systemic effect of high-dose hapten exposure on subsequent sensitization with an optimal dose of hapten.

Mice sensitized with a high dose (3%) of DNFB showed significantly attenuated CHS responses after elicitation compared to mice sensitized with an optimal dose (0.5%) of DNFB (Fig. 1A), which was consistent with a previous report [1]. In addition, CHS responses induced by an optimal dose of DNFB were significantly suppressed in mice pretreated with high-dose DNFB on the abdominal skin one day before sensitization (Fig. 1B–D). To confirm that high-dose DNFB pretreatment inhibited subsequent sensitization with the optimal dose of hapten, CHS transferred via dLN cells of sensitized mice with or without DNFB pretreatment was assessed. Mice subjected to adoptive transfer of dLN cells that had been collected from vehicle-pretreated mice five days after sensitization exhibited substantial CHS responses after elicitation. Mice subjected to adoptive transfer of dLN cells that had been

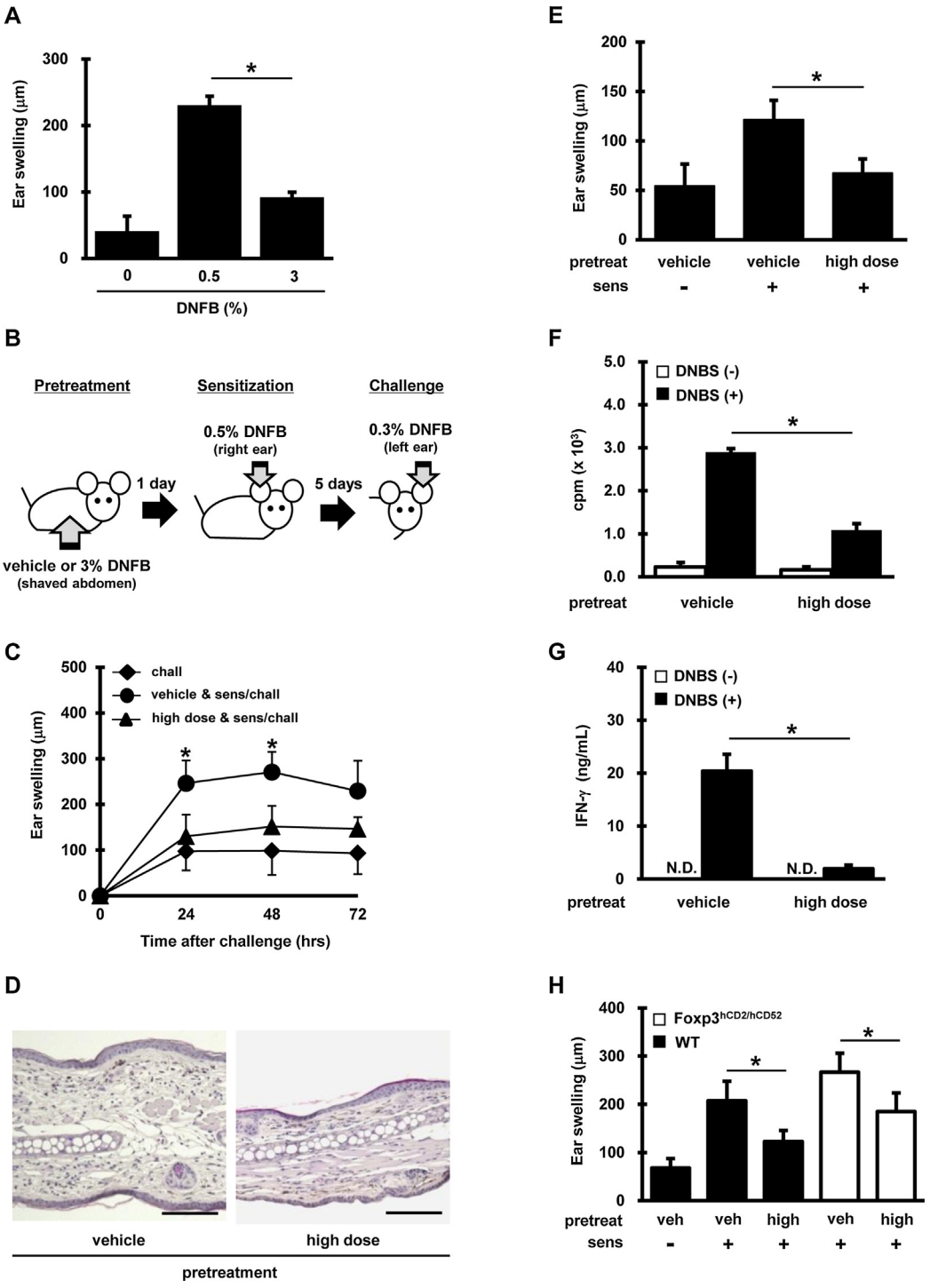

Fig. 1. Topical high-dose DNFB application systemically inhibited subsequent sensitization with an optimal dose of hapten.
(A) CHS was induced with DNFB as previously described [6] with some modifications. C57BL/6 (B6) mice were sensitized with 25 μl of the indicated concentration (v/v) of DNFB onto shaved abdomen and challenged with 20 μl of 0.3% DNFB on each ear 5 days post-sensitization. Ear swelling was measured 24 h after challenge. (B–D) High-dose DNFB pretreatment and CHS induction. (B) Schematic illustration of experimental protocol. B6 mice were sensitized with 20 μl of 0.5% DNFB on right ear one day after pretreatment with 25 μl of vehicle or 3% DNFB onto shaved abdomen, followed by a challenge on left ear as described in A. (C) Ear swelling at 24, 48, and 72 h post-challenge. (D) Hematoxylin and eosin staining of ear sections 24 h post-challenge (scale bar; 100 μm). (E) B6 mice were pretreated and sensitized as described in B. Five days after sensitization, cervical LN cells were removed and adoptively transferred into naïve recipient mice (from two donors to one recipient). Immediately after the cell transfer, the ears were challenged with 0.5% DNFB, and ear swelling was measured 24 h later. (F and G) 2.5×10^5 $CD8^+$ T cells isolated from draining LNs of mice pretreated and sensitized as described in B were stimulated with DNBS (100 μg/mL) in the presence of 5.0×10^5 mitomycin C-treated splenocytes for three days. (F) Cell proliferation was assessed by [^{3}H] thymidine incorporation during the last 24 h. G, The amount of IFN-γ in the culture supernatant was measured by ELISA. N.D., not detected. (H) Effect of $Foxp3^+$ regulatory T-cell depletion on high-dose DNFB-induced suppression of CHS. For selective depletion of $Foxp3^+$ regulatory T cells, $Foxp3^{hCD2/hCD52}$ mice (kindly provided by Dr. Hori), which express human CD2/CD52 fusion protein specifically on cell surfaces of $Foxp3^+$ cells [8], were injected intravenously with anti-human CD2 antibody (clone 35.1). Wild-type (WT) and $Foxp3^{hCD2/hCD52}$ mice were pretreated with vehicle (veh) or 3% DNFB (high), sensitized, and challenged as in B. All mice were injected with anti-human CD2 antibody (0.1 mg/mouse) one day before challenge. Ear swelling was measured 24 h after challenge. Data are shown as the mean ± SD values. Statistical analyses were performed by Student's *t* test. At least four mice per group. $^*p < 0.05$.

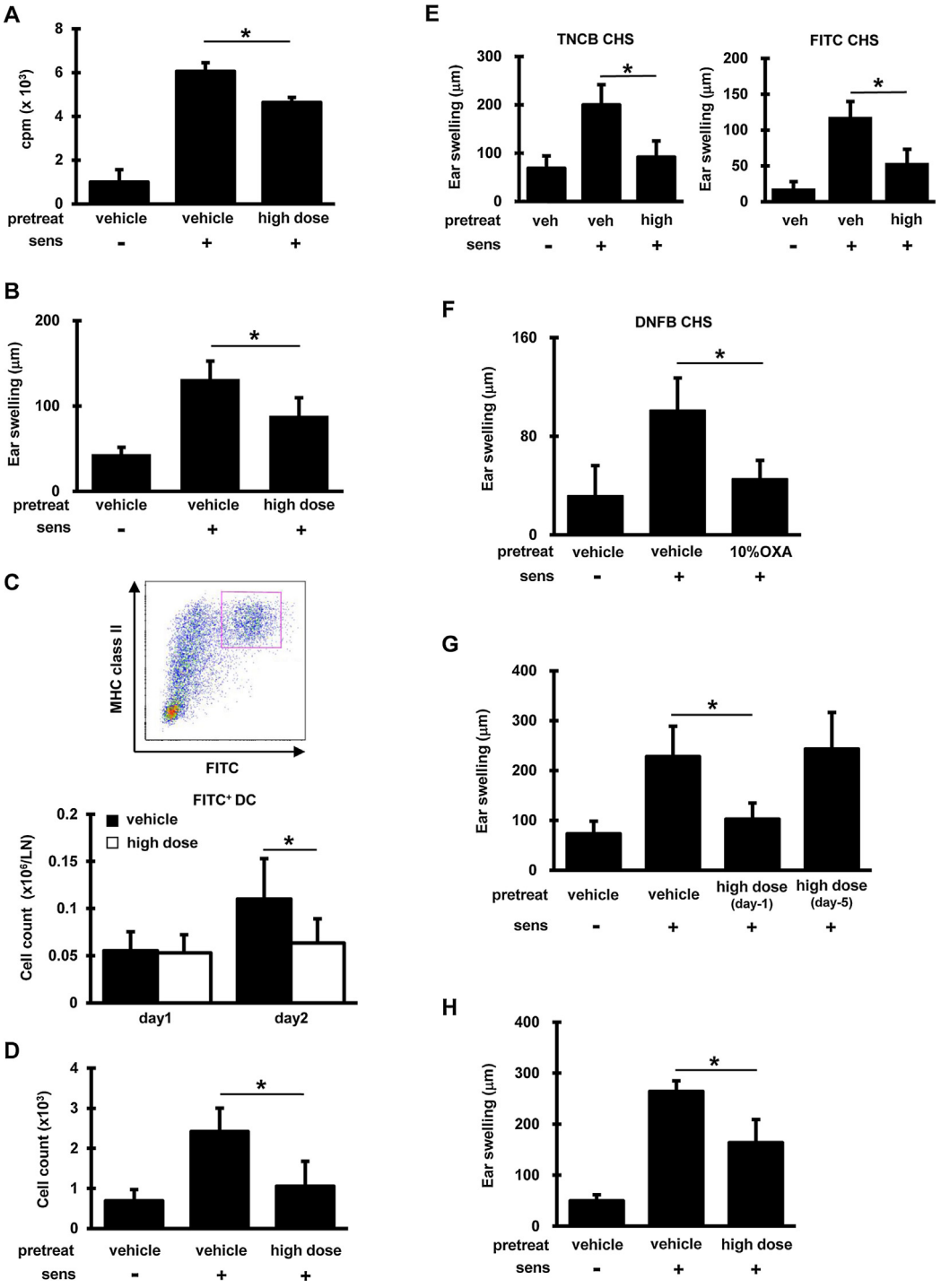

Fig. 2. Percutaneous high-dose DNFB exposure induced systemic inhibition of DC.
(A and B) CD11c$^+$ DCs were isolated from draining LNs of mice pretreated and sensitized as described in Fig. 1B. (A) CD8$^+$ T cells were purified from cervical LNs of mice sensitized with 0.5% DNFB on both ears. 1.0×10^5 CD8$^+$ T cells were cultured with 5.0×10^4 CD11c$^+$ DCs for 3 days. Cell proliferation was measured by [^{3}H] thymidine incorporation during the last 24 h. (B) CD11c$^+$ DCs were injected intradermally into the right ear pinna of naïve recipients (DCs from one donor into one recipient). Five days later, the recipients were challenged with 0.3% DNFB on the left ear. Ear swelling was measured 24 h post-challenge. (C) DC migration assay using FITC. Mice pretreated with vehicle or 3% DNFB were painted with 2% FITC in acetone/dibutylphthalate onto both ears. One or two days later, draining LN cells were analyzed by flow cytometry. Shown is a representative plot of B220-CD11c$^+$ cells from draining LNs of FITC-painted mice, in which the framed rectangle indicates FITC-bearing DCs. The number of FITC-bearing DCs per one draining LN was evaluated. (D) DC migration from ear skin explants. Mice were pretreated and sensitized as described in Fig. 1B. 8-mm punch biopsy specimens were taken from sensitized ears 24 h post-sensitization, split into dorsal and ventral halves, and floated on culture medium for 24 h. The number of CD11c$^+$ cells migrated into culture medium was analyzed by flow cytometry. (E) Mice were pretreated with vehicle (veh) or 3% DNFB (high) onto shaved abdomen. Mice were sensitized with 3% TNCB or 2% FITC one day after the pretreatment, and 5 days later challenged with 1% TNCB or 1% FITC, respectively. (F) Mice were pretreated with vehicle or high-dose (10%) oxazolone (OXA) onto shaved abdomen. Mice were sensitized with 0.5% DNFB one day after the pretreatment, and 5 days later challenged with 0.3% DNFB. (G) Mice were pretreated with vehicle or 3% DNFB onto shaved abdomen one day or 5 days before sensitization with 0.5% DNFB, followed by a challenge with 0.3% DNFB five days post-sensitization. (H) Mice were treated with vehicle or 3% DNFB on shaved abdomen. 24 h later, sera were collected from treated mice and injected intravenously into naïve recipients. Immediately after the serum transfer, recipient mice were sensitized with 0.5% DNFB and challenged with 0.3% DNFB five days after sensitization. Ear swelling was measured 24 h post-challenge. Data are shown as the mean ± SD values. Statistical analyses were performed by Student's t test. At least four mice per group. $^*p < 0.05$.

collected from high-dose DNFB-pretreated mice exhibited only minimal CHS responses (Fig. 1E). To assess the differentiation of antigen-specific Tc1 cells, which are essential for the development of CHS [4], $CD8^+$ T cells purified from the dLNs of sensitized mice were stimulated in vitro with dinitrobenzene sulfonic acid (DNBS), a water-soluble analogue of DNFB. DNBS-induced proliferation and IFN-γ production were markedly lower in $CD8^+$ T cells from high-dose DNFB-pretreated mice than in those from vehicle-pretreated mice (Fig. 1F and G). By contrast, IFN-γ-producing $CD4^+$ T cell differentiation was not impaired in high-dose DNFB-pretreated mice (Fig. S1). These results indicate that pretreatment with high-dose DNFB inhibited subsequent sensitization with an optimal dose of DNFB, probably through impairing the differentiation capacity of antigen-specific Tc1 cells in the dLNs. It is unlikely that $Foxp3^+$ regulatory T cells (Tregs), which have been reported to suppress CHS response [7], contribute to the high-dose DNFB-induced suppression of CHS given that the selective depletion of Tregs *in vivo* one day before elicitation of CHS did not abrogate the suppression (Fig. 1H).

Next, to examine the possibility that the impaired differentiation of antigen-specific Tc1 cells in high-dose DNFB-pretreated mice might be due to dysregulation of antigen-presenting cells, we assessed the T-cell stimulatory capacity of the $CD11c^+$ DC population in the dLNs of sensitized mice with or without high-dose DNFB pretreatment. $CD11c^+$ DCs purified from the dLNs of sensitized mice with high-dose DNFB pretreatment showed significantly attenuated capacity to stimulate $CD8^+$ T cells from DNFB-sensitized mice *in vitro* (Fig. 2A) and to induce sensitization to DNFB *in vivo* (Fig. 2B). *In vivo* DC migration assay using the fluorescent hapten fluorescein isothiocyanate (FITC) revealed that the expected increase in the number of $FITC^+$ DCs in the dLNs after sensitization with FITC was significantly reduced by high-dose DNFB pretreatment (Fig. 2C), indicating that the pretreatment inhibited the migration of antigen-bearing DCs from the sensitized skin to the dLNs. An inhibitory effect of high-dose DNFB pretreatment on cutaneous DC migration was further supported by the finding that, in skin explant culture experiments, the emigration of $CD11c^+$ DCs from the sensitized ear skin into the culture medium was significantly impaired when the sensitized skin was taken from mice pretreated with high-dose DNFB (Fig. 2D). Immunosuppression by high-dose DNFB pretreatment was antigen-nonspecific since CHS responses to TNCB and FITC were also suppressed by pretreatment with high-dose DNFB (Fig. 2E), which was consistent with the aforementioned finding that high-dose DNFB pretreatment inhibited the migration of antigen-bearing cutaneous DCs following sensitization with an irrelevant hapten, FITC (Fig. 2C). In addition, high-dose (10%) oxazolone pretreatment suppressed CHS response to DNFB (Fig. 2F). High-dose DNFB-induced suppression of CHS was not observed when mice were pretreated with high-dose DNFB five days before sensitization (Fig. 2G). CHS responses in mice injected with sera collected from high-dose DNFB-treated mice were significantly attenuated compared to those in mice injected with control sera (Fig. 2H), indicating that this suppression was mediated at least in part by some soluble molecules in the serum. Among the immunomodulatory soluble molecules, interleukin (IL)-10 is well known to suppress DC migration and CHS [9,10]. However, suppression of CHS by high-dose DNFB pretreatment was observed even in IL-10-deficient mice (data not shown), indicating that IL-10 was dispensable for this suppression. Other candidate molecules that may be responsible for this suppression include transforming growth factor beta, prostaglandin E2, vascular endothelial growth factor, and high mobility group box 1.

Taken together, our findings demonstrate that topical application of high-dose hapten systemically suppresses immune reaction to subsequent percutaneous antigen exposure. In addition, underlying mechanisms of the suppression likely include the inhibition of cutaneous DC migration and soluble factors transiently released in the serum shortly after the application of high-dose hapten to the skin.

Conflicts of interest

None.

Funding sources

None

Appendix A. Supplementary data

Supplementary data associated with this article can be found, in the online version, at http://dx.doi.org/10.1016/j.jdermsci.2015.11.011.

References

[1] M.S. Sy, S.D. Miller, H.N. Claman, Immune suppression with supraoptimal doses of antigen in contact sensitivity:I. Demonstration of suppressor cells and their sensitivity to cyclophosphamide, J. Immunol. 119 (1977) 240–244.
[2] P. Phanupak, J.W. Moorhead, H.N. Claman, Tolerance and contact sensitivity to DNFB in mice: III. Transfer of tolerance with suppressor T cells, J Immunol. 113 (1974) 1230–1236.
[3] A. Goubier, B. Dubois, H. Gheit, G. Joubert, F. Villard-Truc, C. Asselin-Paturel, G. Trinchieri, D. Kaiserlian, Plasmacytoid dendritic cells mediate oral tolerance, Immunity 29 (2008) 464–475.
[4] T. Honda, G. Egawa, S. Grabbe, K. Kabashima, Update of immune events in the murine contact hypersensitivity model: toward the understanding of allergic contact dermatitis, J. Invest. Dermatol. 133 (2013) 303–315.
[5] S. Bacci, P. Alard, R. Dai, T. Nakamura, J.W. Streilein, High and low doses of haptens dictate whether dermal or epidermal antigen-presenting cells promote contact hypersensitivity, Eur. J. Immunol. 27 (1997) 442–448.
[6] Y.L. Shi, J. Gu, J.J. Park, Y.P. Xu, F.S. Yu, L. Zhou, Q.S. Mi, Histone deacetylases inhibitor Trichostatin A ameliorates DNFB-induced allergic contact dermatitis and reduces epidermal Langerhans cells in mice, J. Dermatol. Sci. 68 (2012) 99–107.
[7] T. Honda, Y. Miyachi, K. Kabashima, T. Regulatory, cells in cutaneous immune responses, J. Dermatol. Sci. 63 (2011) 75–82.
[8] N. Komatsu, M.E. Mariotti-Ferrandiz, Y. Wang, B. Malissen, H. Waldmann, S. Hori, Heterogeneity of natural Foxp3+ T cells: a committed regulatory T-cell lineage and an uncommitted minor population retaining plasticity, Proc. Natl. Acad. Sci. U. S. A. 106 (2009) 1903–1908.
[9] B. Wang, L. Zhuang, H. Fujisawa, G.A. Shinder, C. Feliciani, G.M. Shivji, H. Suzuki, P. Amerio, P. Toto, D.N. Sauder, Enhanced epidermal Langerhans cell migration in IL-10 knockout mice, J. Immunol. 162 (1999) 277–283.
[10] A.H. Enk, J. Saloga, D. Becker, M. Mohamadzadeh, J. Knop, Induction of hapten-specific tolerance by interleukin 10 in vivo, J. Exp. Med. 179 (1994) 1397–1402.

Kazutoshi Saito[a,b]
[a]Department of Dermatology, Kyoto University Graduate School of Medicine, Kyoto, Japan, [b]Kao Corporation, R&D Safety Science Research, Tochigi, Japan

Akihiko Kitoh[**], Sho Hanakawa
Department of Dermatology, Kyoto University Graduate School of Medicine, 54 Shogoin Kawara, Sakyo, Kyoto 606-8507, Japan

Takashi Nomura[a,b]
[a]Department of Dermatology, Kyoto University Graduate School of Medicine, Kyoto, Japan, [b]Department of Dermatology, Ijinkai Takeda General Hospital, Kyoto, Japan

Yoshiki Miyachi[a,b]
[a]Department of Dermatology, Kyoto University Graduate School of Medicine, Kyoto, Japan, [b]Shiga Medical Center for Adults, Shiga, Japan

Kenji Kabashima[a,b,c,*]
[a]Department of Dermatology, Kyoto University Graduate School of Medicine, Kyoto, Japan, [b]Singapore Immunology Network (SIgN) and Institute of Medical Biology, Agency for Science, Technology and Research (A*STAR), 8A Biomedical Grove, IMMUNOS Building #3-4, Biopolis 138648 Singapore, [c]PRESTO, Japan Science and Technology Agency, 4-1-8 Honcho, Kawaguchi, Saitama 332-0012, Japan

** Corresponding author. Fax: +81 75 761 3002.

* Corresponding author. Fax: +81 75 761 3002.
E-mail addresses: kichu@kuhp.kyoto-u.ac.jp (A. Kitoh), kaba@kuhp.kyoto-u.ac.jp (K. Kabashima).

Received 14 October 2015
Received in revised form 17 November 2015
Accepted 26 November 2015

http://dx.doi.org/10.1016/j.jdermsci.2015.11.011

Letter to the Editor

Genetic analyses of oculocutaneous albinism types 2 and 4 with eight novel mutations

Oculocutaneous albinism (OCA), inherited as an autosomal-recessive trait, is characterized by reduction or absence of melanin in the skin, hair, and eyes. OCA patients show symptoms such as reduced skin and hair pigmentation and consequent photosensitivity, high risk of skin cancer, and reduced visual acuity and nystagmus [1]. OCA is broadly classified into two groups: non-syndromic and syndromic, based on the presence of other symptoms such as bleeding diathesis, immunodeficiency, or neurological dysfunction [2]. OCA type 2 (OCA2, Online Mendelian Inheritance in Man [OMIM] #203200) caused by mutations in *P (OCA2)* [3] is the most common type of OCA worldwide (accounting for approximately 50% of all patients with OCA); however, the frequency among Japanese OCA patients is less than 10% [1]. On the other hand, OCA type 4 (OCA4, OMIM #611409) caused by mutations in *SLC45A2* [4] is rare worldwide, while in Japanese OCA patients, the frequency of OCA type 4 is approximately 30% [5]. Both, OCA2 and SLC45A2 proteins contain 12 putative transmembrane domains and are thought to function as transporters. Most pathological missense substitutions for albinism are located within or in close proximity to these domains [1], indicating that they play a critical role in overall protein function. These two subtypes show high clinical heterogeneity, from mild to severe hypopigmentation and a genotype-phenotype relationship has been previously reported. For example, p.A481T mutation in *OCA2*, located distal to the transmembrane domain, is reportedly associated with the mild phenotype. This pathogenic variant, which has 70% melanogenesis activity, has been found in not only OCA2 patients but also in approximately 12% of normally pigmented Japanese [1]. Recent investigations on *OCA2* in the Japanese population have also shown that p.A481T and p.H615R substitutions significantly contribute to skin color and are associated with risk of skin cancer [6,7]. Meanwhile, Shimanuki et al. [8] indicated that some *OCA2* variations including p.A481T, may have developed via diversifying selection.

We had the opportunity to examine seven Japanese patients with non-consanguineous parents, who were clinically diagnosed with OCA. Informed consent and blood samples were obtained following protocols approved by the Ethics Committee of Yamagata University, Faculty of Medicine. Samples were screened for *TYR* (OCA1), *P* (OCA2), *TYRP1* (OCA3), *SLC45A2*(OCA4), and *HPS1*(HPS1) mutations using single-strand conformation polymorphism/heteroduplex and direct sequencing techniques as previously described [5]. This analysis allowed us to genetically diagnose the subtypes of OCA and resulted in the detection of eight novel mutations (Table 1). These mutations included two splice-site mutations, IVS13 + 1(c.1364 + 1)G > A and IVS19 + 1(c.2079 + 1)G > A in *OCA2* (GenBank Accession number: NM_000275.2); five missense mutations, (c.125T > C, p.M42T; c.149C > T, p.A50V; c.157G > C, p.A53P; c.170C > T, p.T57I; and c.217G > T, p.V73L); and one nonsense mutation, c.1030C > T, p.Q344X in *SLC45A2* (GenBank Accession number: NM_016180.3). The newly identified mutations were not found in 100 unrelated, normally pigmented Japanese adults and were not identified in the 1000 Genomes Project and single nucleotide polymorphism (dbSNP, Build 142) databases. We confirmed that all the amino acids altered by these missense mutations were conserved among species including chimpanzee, monkey, cow, mouse, chicken, zebrafish, and frog. In addition, the novel missense mutations in *SLC45A2*, all of which were located within the transmembrane domain, were analyzed by nine different algorithms used to evaluate the functional impact of a variation: SIFT, PolyPhen2 based on HumanDiv and HumanVar models, LRT, Mutation Taster, Mutation Assessor, FATHMM, MetaSVM and MetaLR scores provided by dbNSFP 2.3 [9]. At least seven of the nine algorithms predicted these variations to be “damaging” or “probably damaging” (9/9: p.A50V, p.A53P, p.T57I; 8/9: p.M42T; 7/9: p.V73L). These findings indicated that the mutations are likely not polymorphisms and are probably pathological. Patients carrying these mutations (patients 3–6 showed compound heterozygous missense mutations) revealed some phenotype heterogeneity, indicating that aberrant proteins induced by missense substitutions resulted in variable loss of functional activity.

In addition, in the two cases with splice-site mutations in *OCA2*, we investigated effects of nucleotide changes at the splice site on the pre-mRNA splice pattern, using reverse-transcriptase polymerase chain reaction (RT-PCR) with RNA extracted from peripheral blood as previously described [10]. The primers used for RT-PCR were EX11cf (5′ CATGTGGTGGAGTGGATTGA 3′) and EX15cr (5′ AGTGAATCCGGCAAAGTCC 3′) for samples from patient 1, and EX18cf (5′ CAAATGCCTGACAGTGTTGG 3′) and EX21cr (5′ GGTAGCAGTGAACGGGATGT 3′) for samples from patient 2. DNA sequencing of the RT-PCR product of the samples obtained from patient 1 revealed a 92-nucleotide addition within exon 13 (Fig. 1a), predicted to cause a frameshift that encoded a truncated peptide with an additional 43-amino-acid peptide (p.R455fsX499). In patient 2, a skipping of exon19 was confirmed (Fig. 1b). This skipping is predicted to result in a frameshift and a truncated protein with an additional 45-amino-acid peptide (p.G651fsX697). Interestingly, one allele from patient 1 with relatively mild phenotype contained two missense substitutions (p.R10W and p.A481T) inherited from her mother, while another allele contained a splicing mutation that would result in a frameshift and a truncated protein, indicating the former allele retained some functional melanogenesis activity despite the combination of two pathological substitutions.